Influences of Vibration Exposure on Battery Pack for Two-Wheeler Electric Vehicles

Mohamad Ardy Firmansyah
Mechanical Engineering Department, Mercu Buana University

Ruhyat, Nanang
Mechanical Engineering Department, Mercu Buana University

Firdaus, Himma
Research Center for Testing Technology and Standard, BRIN

https://doi.org/10.5109/7236909

出版情報：Evergreen. 11 (3), pp.2700-2710, 2024-09. 九州大学グリーンテクノロジー研究教育センター
バージョン：

Influences of Vibration Exposure on Battery Pack for Two-Wheeler Electric Vehicles

Mohamad Ardy Firmansyah[1,2,*], Nanang Ruhyat[1], Himma Firdaus[3,4]
[1]Mechanical Engineering Department, Mercu Buana University, Indonesia
[2]Vehicle Testing and Certification Centre Ministry of Transportation Republic Indonesia, Indonesia
[3]Research Center for Testing Technology and Standard, BRIN, Indonesia
[4]Electrical Engineering Department, Pamulang University, Indonesia

*Author to whom correspondence should be addressed:
E-mail: 55822120004@students.mercubuana.ac.id, mohamad_ardy@dephub.go.id

(Received May 10, 2024: Revised May 29, 2024: Accepted August 2, 2024).

Abstract: This study investigates the structural protection level of battery packs for two-wheeler electric vehicles due to vibration exposure. The research comprises two phases: first, an exploration of resonance frequencies in both the fixture and the battery pack, followed by vibration testing using the UN ECE R136 test profile encompassing a frequency range of 7-200 Hz and acceleration between 10-80 m/s^2. These tests are designed to emulate the vibration exposure experienced by two-wheeler electric vehicle batteries during typical operation. The vibration cycle is repeated seven times, and after each cycle, an assessment of the battery pack structure is conducted, utilizing a 72 Volt 20 Ah Li-ion electric motorcycle battery pack as a test sample. The results reveal that the battery pack suffered resonances at 28 Hz, resulting in an acceleration amplification exceeding 40% of the applied vibration exposure and a total force of up to 226.95 N pressing on the battery structure. The resonance severely damages all four elastic foundations and the BMS holder supporting the upper battery structure. These findings emphasize the imperative for further research into battery pack structures for two-wheeler electric vehicles capable of withstanding resonance in all testing conditions, ensuring the battery pack's safety and durability.

Keywords: Lithium Ion; Vibration Test; Resonance; Acceleration Amplification

1. Introduction

The Indonesian Government is committed to achieving Net Zero Emissions by 2060[1–4] aligning with global efforts to reduce transportation emissions by transitioning from internal combustion engine vehicles to electric vehicles[5]. In the first semester of 2023, Indonesia experienced a remarkable 1000% increase in its electric vehicle population[6]. Despite this significant growth, the transition to electric vehicles in the country encounters various challenges, resulting in a low adoption rate of merely 0.3%[7]. The problems include reliance on imported components, industry reluctance, operational obstacles such as safety concerns in waterlogged areas, limited battery capacities, and various battery risks like explosions, fires, and vibrations[8,9]. Battery performance and safety are the biggest challenges for implementing electric vehicles.

Most of the main components of electric vehicles in Indonesia, including batteries, have been imported[10]. Before vehicles are mass-produced, imported, and assembled, the Indonesian Ministry of Transportation or other government authorities must conduct a vehicle certification process. Complete testing of electric vehicles (EVs) should be performed by an institution called the Vehicle Testing and Certification Center to ensure their performance and safety. However, it is noteworthy that the battery pack, a critical component in an EV, is currently not subjected to direct testing but relies on a submitted test report scheme from its country of origin. This research underscores the significance of implementing standardized testing protocols for battery packs, especially for vibration testing. The aim is to encourage government authorities and private laboratories to undertake thorough assessments of battery packs, ensuring adherence to the established standards. It also plays a crucial role in supporting the ASEAN Automotive Committee in enhancing laboratory competence for conducting battery testing adhering to the international standard.

Battery testing for electric vehicles (EVs) is guided by various international standards. The IEC 62660 series covers performance, reliability, and abuse resistance of lithium-ion cells. ISO standards, such as ISO 12405-4:2018, address performance tests for traction battery packs and systems. UN ECE regulations, like UN ECE

R100 and UN ECE R136, set safety requirements for Rechargeable Electrical Energy Storage Systems (REESS) in road vehicles and light vehicles. The standards require vibration test both for performance and safety aspects. This research focuses on UN ECE R136 due to its specific emphasis on L-category vehicles including two-wheeled EVs for safety concern, addressing their unique challenges such as higher exposure to vibrations and mechanical stresses.

According to UN ECE R136, vibration testing is crucial for vehicle certification, along with thermal shock, drop, force charge, force discharge, and external short circuit testing[12)13)]. The vibration test profile in testing standards is developed to verify the safety and performance of the battery under a vibration environment, which the battery will experience during normal operation. The test profile accelerates the battery's vibration exposure over a 15-year electric vehicle life cycle (60,000 miles)[14)] in a short testing duration. This standard highlights the significance of vibration testing, which refers to the standard in assessing the safety and performance of lithium-ion battery packs.

As mentioned above, vibration inherent to moving or rotating structures and systems remains an undeniable physical phenomenon arising from rotor imbalances or irregular road surfaces[15)]. This phenomenon notably affects electric vehicle (EV) batteries during on-road operations[16,17)]. Its impact has been extensively detailed in prior studies, where vibration tests on 32-cell batteries revealed a drop in capacity from an initial range of 2930 – 3065 mAh to 2854 – 3016 mAh after the post-test. There was also an increase in the internal resistance of the 26-cell batteries, which is detrimental to lithium-ion batteries[18)]. Vibration testing affected structural stiffness, and cell amplitude changed when vibration testing was subjected to 18650 lithium-ion cells[19)].

Meanwhile, dynamic and vibration loading tests on lithium batteries have been examined, and the results of the pouch cells do not show degradation or failure in any tests. However, the y direction of the mandrel experiences loosening during long-term shock and vibration tests. In addition, it was found that cylindrical cells that were stressed in the z direction also experienced degradation and failure. For example, after ten applications of sine vibration, a loose mandrel was found when the cell was removed from the test apparatus, even though capacity measurements could not detect degradation. In the shock test, no degradation was initially detected in the capacity determination; however, images collected before and after testing showed that the circuit breaker device (CID), which helps regulate pressure inside the cell, was damaged[20)].

In addition, a loose mandrel, which was in contact with the current collector and CID, was also observed. This finding is important because it shows that although the cells appear intact from the outside and have passed standard tests, they are near a failure state internally. Loose mandrels are also observed at the end of long-term vibration tests, and as mentioned previously, the mandrels may meet the terminals. Subsequent scanning electron microscope imaging showed a damaged separator, causing an internal short circuit [1)]. There was a release of the mandrel on two types of batteries, namely Samsung INR 18650-35E and Samsung ICR18650-22FM, after vibration testing, where the battery mandrel is an essential component in a lithium-ion battery as the core or central core of the battery and functions as a jelly roll stabilizer in the battery during operation under dynamic conditions such as vibration or shock. However, not all brands of lithium-ion batteries have a mandrel as the core of the lithium-ion battery[21)].

Apart from the research results above, the authors have compiled at least three cases regarding air cargo accidents. In August 2009, FedEx indicated smoke and fire in packages containing 33 GPS Trackers, indicating the causes were vibration, external short circuits, and poor gasket. Another incident in the same month involved a UPS that caught fire containing batteries at the Taiwan air terminal due to an external short circuit and mechanical vibration. In June 2009, an e-bike battery in Honolulu experienced overheating. The battery was packaged using only bubble wrap and cardboard, leading to external short circuits and vibrations[22)23)].

Previous research focuses on examining battery cells rather than battery packs[14,18–21)]. Li et al.'s study[24)] is an exception, as it analyzed battery packs as integral units in electric vehicles. However, the study was limited to highway vibration exposure and analyzed only the effect on battery cells. This approach may not holistically represent electric vehicle operations since the vehicles are exposed to various street vibration conditions. Furthermore, the battery encompasses multiple components, such as casing, battery holder, battery cells, battery management system, connectors, fuses, and more, integrated into a singular unit.

In the evaluation of vibration test, resonance plays a pivotal role, occurring when a structure vibrates in response to external influences at its natural frequencies[25)]. Past studies successfully mitigated resonance by altering vibration characteristics, specifically natural frequency and response strengthening, redirecting its impact away from the structure. The effort was applied to a vehicle's active suspension at the driver's seat so that a greater comfort level was obtained[26)]. Resonance also disrupts structures; reportedly, resonance amplifies the load by 100 to 1000 times greater than the static load[27)].

Based on the research findings, as mentioned earlier, there is a noticeable gap in comprehensive studies focusing on battery packs' resilience and mechanical integrity for two-wheeler EVs when exposed to standardized vibration test profiles. Furthermore, according to the authors' knowledge, no comprehensive work has been dedicated to thoroughly analyzing the resonance frequencies of battery packs and their structural integrity under these conditions. Therefore, the research aims to comprehensively understand and enhance the resilience of the battery packs by investigating their dynamics under vibration exposure adhering to UN ECE R136. The study also identifies resonance and potential damage to the battery pack under specific testing conditions, emphasizing the importance of further optimization in design and testing protocols.

2. Research Methodology

In this research, the investigation of battery pack dynamics is conducted through a multifaceted approach encompassing theoretical modeling and practical experimentation. The elucidation of the battery pack's behavior and resilience under vibration exposure involves an integration of vibration theory principles and experimental testing methodologies. The following subsections delineate the comprehensive methodology employed, commencing with an exploration of the spring model theory applied to battery pack dynamics (Section 2.1), followed by an intricate delineation of the test methods utilized to assess the structural integrity of battery packs under defined vibration conditions (Section 2.2). This comprehensive approach ensures a thorough understanding of the battery pack's response to vibrations and paves the way for enhancing its durability and safety in two-wheeler electric vehicles. The methodology in this research employs a qualitative approach involving a general assessment of the battery pack's performance in safeguarding the enclosed battery cells and maintaining its structural integrity. Various parameters, including the fundamental characteristics of the vibration equation, such as displacement, speed, and acceleration in battery cells, are considered crucial. This importance stems from the ability of these parameters to indicate the extent to which battery cells experience shaking during the vibration testing process of the battery pack[24].

2.1 Spring model of a battery pack

The spring model applied to battery pack dynamics in this research is drawn from pertinent literature on vibration theory. The spring here is an assumption for the elastic foundation in the battery pack. The elastic foundation has an effect in minimizing the vibrations received[25]. According to vibration theory, this elastic foundation is analogized as a spring, while the battery components (battery, battery holder, BMS, and BMS holder) are considered spring masses. The side, top, and bottom battery covers are assumed to be grounded. This assumption is also used as the basis for a framework for testing lithium-ion batteries, where the case is considered masses 1 and 4, and the battery cells are considered masses 2 and 3. In contrast, the viscous fluid is considered k or spring and c or shock absorber[24]. Battery visualization and the spring mechanism - the spring-loaded mass is shown in Fig. 1.

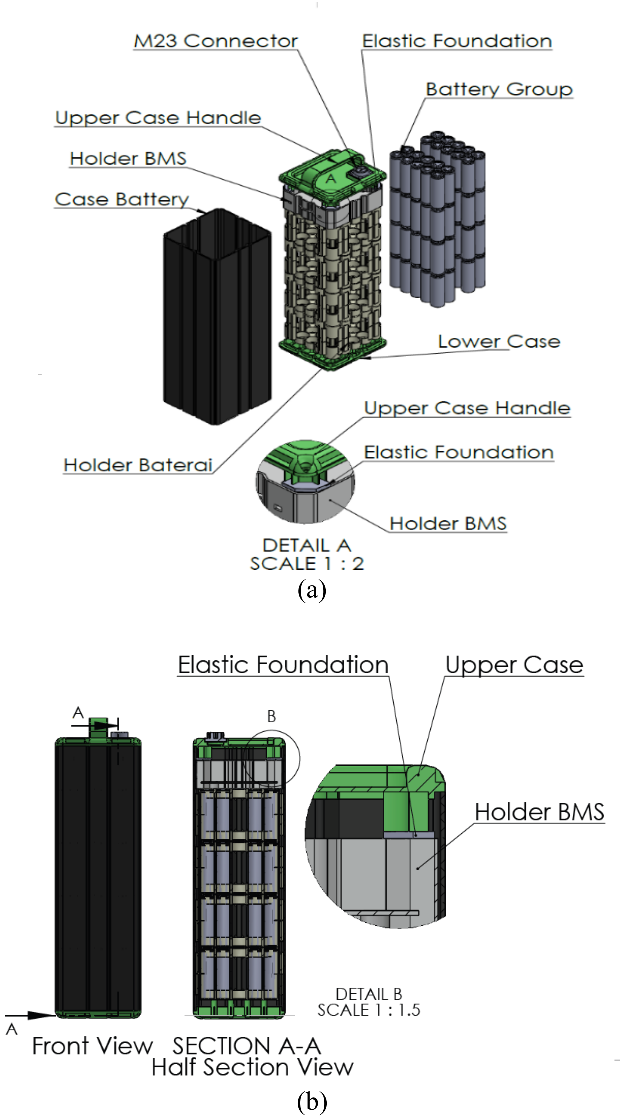

Fig.1. (a) Isometric View Lithium Ion Battery 72 Volt 20 Ah, **(b)** Front and Half Section View Lithium Ion Battery 72 Volt 20 Ah

In the mechanical arrangement shown in Fig. 1, we can arrange the composition in the mechanical vibration theory below.

The general vibration formula that will be used from the conditions mentioned above can be formulated as follows.

- Spring stiffness theory states that the force (F) applied to an object will be directly proportional to the multiplication of the stiffness value (k) of the spring itself with the total deflection (x) that occurs.

$$F = kx \quad (1)$$

- Natural frequencies are analyzed to find out where resonance will occur. The natural frequency is denoted by the formula for spring stiffness (k) and the mass of the spring structure (m).

$$Wn = 0.5\,\pi^{-1}\left[\frac{k}{m}\right]^{0.5} \quad (2)$$

As assumed in Figure 2, the ground and spring-mass weighing is as follows.

- The total mass of the battery = 8.128 kg

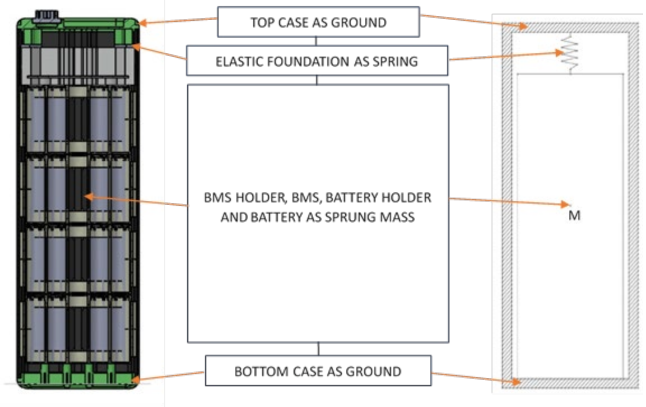

Fig. 2. Assumptions of battery mechanical arrangement in the case of mechanical vibration

- Spring mass (MS) = 6.610 kg; spring mass includes 80 battery cells, battery holder, BMS, and BMS holder. They are tied together in a single structure using a long bolt.
- Battery unsprung mass (MUS1) = 1.518 kg. The battery's unsprung mass includes a side aluminum casing, a top casing, and a bottom casing.
- The unsprung mass of the battery fixture (MUS2) = 1.969 kg. This mass includes the retaining jig and the battery fastening bolt mechanism with the shaker table.
- Total unsprung mass (MUS) = 3.487 kg

We can arrange the mass and spring schematic configuration in Fig. 3 with the weighing data above.

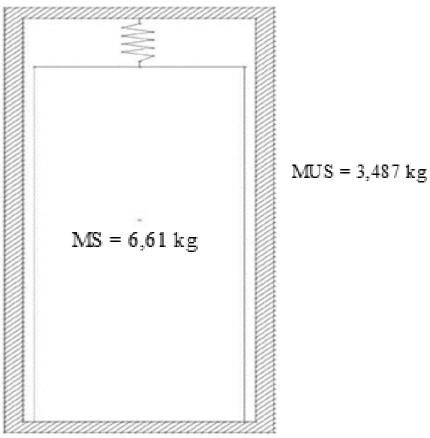

Fig. 3. Spring and groundmass schematic with known values

The battery pack specifications are as follows:

- Nominal Voltage = 72 Volt DC
- Nominal Capacity = 20 Ah
- Type = Lithium Ion
- Configuration = 20 Seri 4 Parallel (80 Cells).

The battery cell specifications are :

- Nominal Voltage = 3.6 Volt DC
- Nominal Capacity = 5 Ah
- Max Charging Current: 0-25C @1.455A, 25-45C @3.395A
- Max Continuous Discharging Current: 7.275A
- Dimensions: 70.8mm (L) x 21.44 mm (D)
- Weight (max): 70.0g.

2.2 Test Method

The test method conducted in this study involves two main phases to evaluate the structural integrity of battery packs for two-wheeler electric vehicles under vibration exposure. Initially, resonance frequencies were investigated within the fixture and the battery pack to evaluate the system's rigidity. The investigation into resonance frequencies was conducted within a frequency range spanning from 5 to 200 Hz, applying an acceleration of 1 G to both the test fixture and the battery pack. This meticulous examination aimed to identify specific frequencies at which the structure exhibited resonance tendencies, providing crucial insights into the vulnerability of the test fixture and the battery pack under various vibration conditions. This range of frequencies and the consistent acceleration ensured a comprehensive assessment, enabling the precise identification of resonance points crucial for understanding and fortifying the structural integrity of the battery pack and the fixture.

Secondly, the battery pack was exposed by a vibration test with a vibration profile adapted from the UN ECE R136 Part 2 vibration test method. The test setup for vibration testing based on this standard is described as follows.

- Frequency and acceleration usage table. For batteries with a mass of less than 12 kg, table 1 in Annex 8A of the rules is selected:

Table 1 Frequency and Acceleration (gross mass of tested device less than 12 kg)

Frequency [Hz]	Acceleration [m/s^2]
7 – 18	10
18 – approximately 50	Gradually increased from 10 to 80
50 - 200	80

Amplitude is maintained at 0.8 mm (1.6 total steps)

- Test the setup on the test bench.

The test object will be rigidly attached to the test bench with the help of a set of jigs, as shown in Fig. 3. The test object will be tested on the z-axis or up and down axis. The setup adapts to the actual condition of the motorbike battery, which is installed in a standing position on the motorbike.

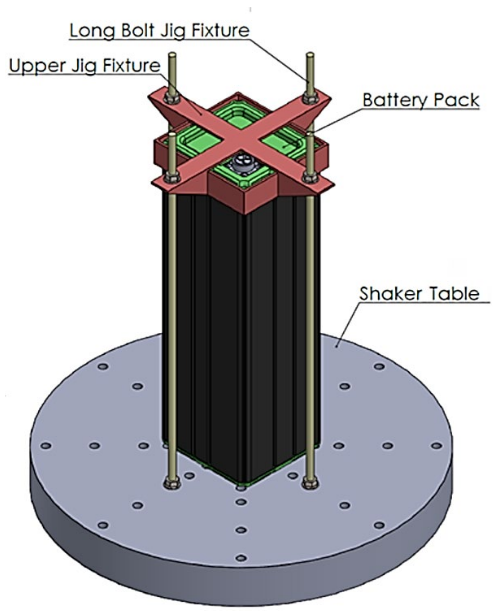

Fig. 4. Test Set Up

- The state of charge must be above 50%. In this case, the test is carried out with a state of charge of 100%.

After weighing the structure to be assumed, battery vibration testing was carried out according to the scheme in Fig. 4. Fig. 5 below shows a picture of the test preparation and battery vibration testing processes.

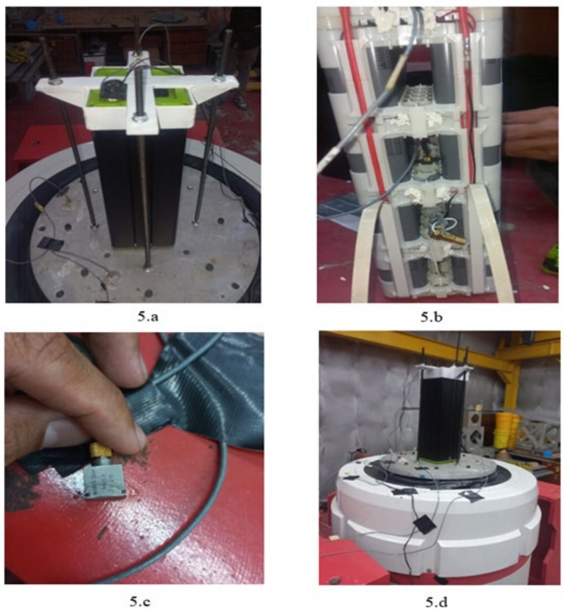

Fig.5.a The installation of transducer 4 in the fixture, **5.b** Installation of transducer 3 in the center of gravity (CoG) of the battery cell, **5.c** Vibration transducer, **5.d** Setup of vibration testing on a table shaker.

The test apparatus used in this work includes the table shaker LDS V850-440, which has a maximum acceleration of 95 g and a usable frequency range of 5-3000 Hz. It also features the Bruel Kjaer 4508-B Transducer, weighing 4.8 grams, with a frequency range of 5000 Hz and a maximum acceleration of 70 g. Additionally, we utilized Shaker Control Software for pre- and post-processing. Figure 6 described how we made an experimental set up for this work.

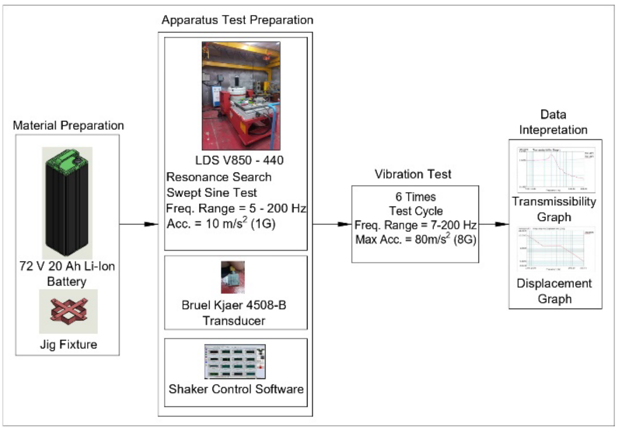

Fig. 6. Eksperimental Set Up

3. Results and Discussion

Vibration testing of the battery pack was initially performed by swept sine test with a test profile frequency range of 5-200 Hz and an acceleration of 1G. The swept test was essential to assess how well the fixture had been designed to hold the battery pack in the planned test. The swept test is carried out for safety considerations for vibration testing in the laboratory. The transmissibility graph for the test is depicted in Fig.7. Figure 7 outlines a resonance frequency at 158 Hz alongside a transmissibility level (ratio between fixture acceleration and controlled acceleration) below 2, signifying the fixture's response to vibrations within this frequency range[28)]. The response indicates that the energy transferred through the system remains relatively low at this specific frequency, suggesting a level of damping or reduced amplification of vibrations within the fixture[29)]. The resonance frequency, located at 158 Hz, is a critical insight as it signifies the point at which the fixture is most susceptible to vibrational excitation, potentially causing structural stress or damage. However, the transmissibility below 2 denotes that the system exhibits a relatively controlled response at this frequency, implying a certain level of stability or mitigation in the transmitted vibration energy. There is no resonance frequency of the fixture below 100 Hz.

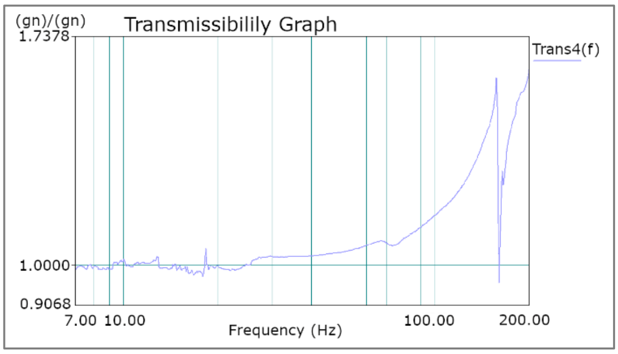

Fig. 7. Transmissibility graph for the resonance frequency of the battery fixture

After the swept test is carried out, testing is then carried out by the UN ECE R136 test profile, namely vibration testing with a peak frequency of 200 Hz and peak acceleration of 8G for 15 minutes, which is repeated for six cycles. The author considers only six testing cycles, which is half of the total cycles required, namely 12 cycles, because, after six testing cycles, the graphic plots obtained are similar between cycles.

The graphic plots obtained for the first to sixth test are shown in Fig. 8.

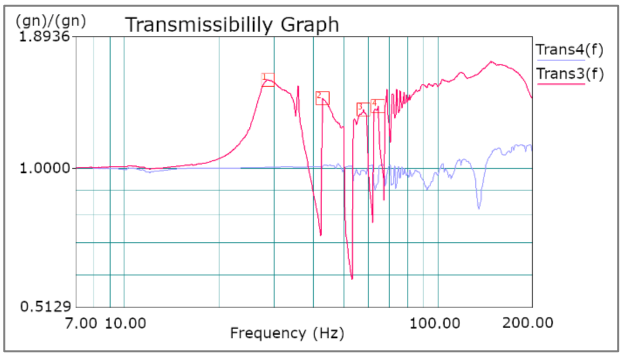

(a)

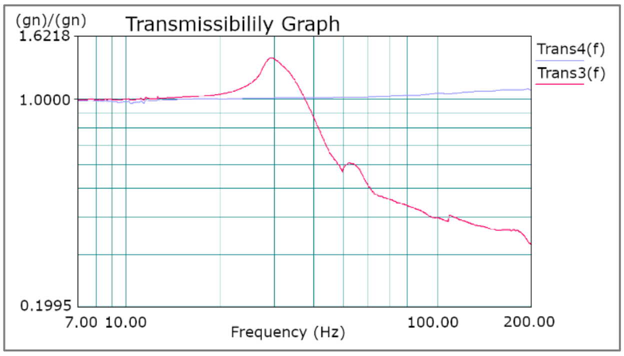

(b)

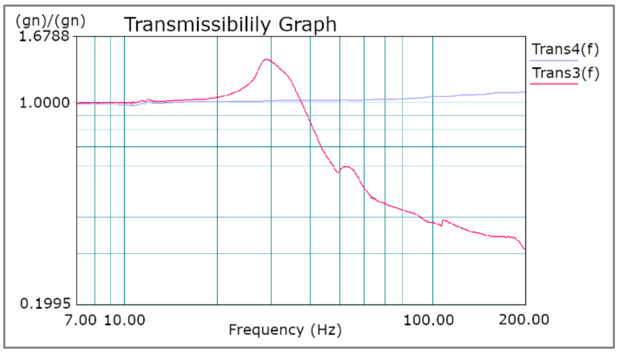

(c)

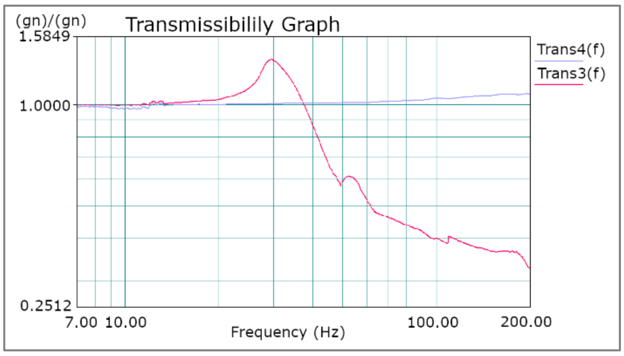

(d)

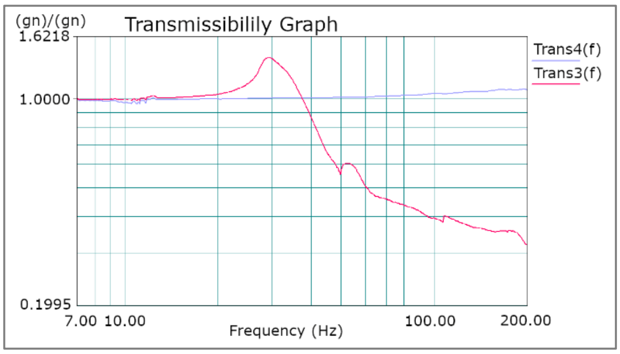

(e)

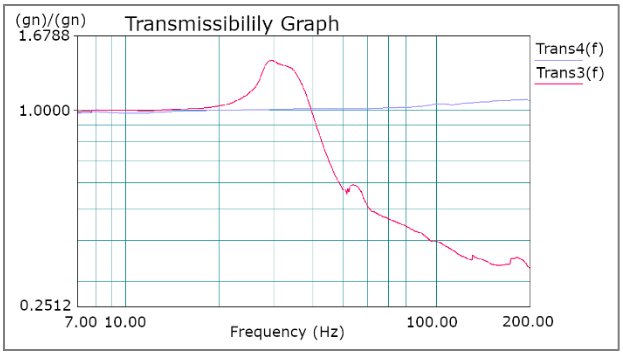

(f)

Figure 8. (a)- (f) Frequency vs Transmissibility Graph Plot of the first to sixth test, Trans4 (f) is response for the accelerometer (transducer) installed on the fixture, and Trans3(f) is the response for those inside the battery pack.

When compared to Fig. 7 and 8, it can be seen that fixture vibration has underdamped at its resonance frequency and gained transmissibility below 1.1 after battery installation due to the high sprung mass of the battery. It indicated that the resonance of the fixture less affected the battery structure.

The analysis results of the six graphs can be outlined in the following description. There is a significant difference between the first and second tests, while the second and sixth tests show similar graphic plots. In the first test, the fixture fastening bolts were loosening, which affected the number of resonances. Four resonances were recorded that occurred at frequencies of 28, 42, 57, and 64 Hz, respectively. A similar graphic plot appears after tightening the fixture fastening bolts before each cycle starts. The transmissibility graph compares the acceleration input provided by the vibration test tool, namely the shaker table, to the acceleration response sensed via the transducer in Fig. 5.c.

According to Fig. 8, the value of transducer four does not change significantly from 1, only increasing slightly to around 1.1 at a frequency of 200. It shows that the stiffness of the fixture is close to the ideal value where the fixture should move, have a speed, and have the same acceleration as the table shaker. Meanwhile, transducer 3 has the highest fluctuating value at around 28 Hz with a gn/gn value of 1.3 – 1.4 and the lowest at a frequency of 200 Hz with a gn/gn value of 0.33. From this analysis, we can judge that resonance occurs at 28 Hz. At a frequency of 28 Hz, the acceleration value is around 2.5 G or 24.525 m/s^2, but because there is resonance, the value is amplified by 1.4 times to become 34.335 m/s2. Resonance in the battery structure will be detrimental to the battery itself because the higher the acceleration value, the higher the force exerted on the structure. If we use an unsprung mass value of 6.61 kg with an acceleration value of 34.335 m/s^2, we get a force of 226.95 N pressing on the battery structure.

Meanwhile, at the peak frequency, namely 200 Hz, there is a G value ranging from 0.33 x 8 x 9.81 m/s^2 = 25.898 m/s^2. If the spring mass is multiplied, the force obtained is 25.898 m/s^2 multiplied by 6.61 kg = 171.18 N. It gives an idea: no significant force is pressing on the battery at the peak frequency (200 Hz) and the peak acceleration (8G). Instead, there is a frequency of 28 Hz, 226.95 N.

Henceforth, from the six experiments testing vibration frequencies above 37 Hz, the gn/gn value was smaller than 1. This means that transducer 3 accelerated less than the acceleration carried out by the table shaker. This shows that a frequency of 37 to 200 Hz is safe for testing battery packs and has a less damaging effect. In line with this research, there is a similarity with previous research, which studied the resonance frequency of satellite antennas that carried out vibration testing at the base. It resonated at 40 Hz while the peak frequency in the test was 100 Hz; at 40 Hz, it produced an acceleration with a value of 4.8G. Compared with other conditions, the acceleration value is below 0.5G in all conditions. This research is similar to previous research, which studied the resonance frequency of satellite antennas and carried out vibration testing at the base of the antenna. It resonated at 40 Hz, while the peak frequency in the test was 100 Hz. At a frequency of 40 Hz, it produced an acceleration with a value of 4.8G, while in average conditions, the acceleration value is below 0.5G. This result is presented in Fig. 9[30].

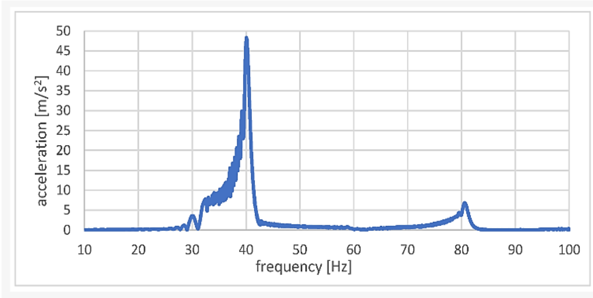

Fig. 9. Plot graph vibration test for satellite antennas

In another study, mounting performance in battery vibration testing was compared using different types of mounting, including electromagnetic, vacuum, and bolt. It was found that bolts, which are a traditional method of tightening, provide the highest clamp strength. The transmissibility caused by bolt tightening is very similar to the current work, starting at a frequency of 5Hz and slightly increasing to 200Hz by the end of the test. These findings are detailed in Fig. 10.[31]

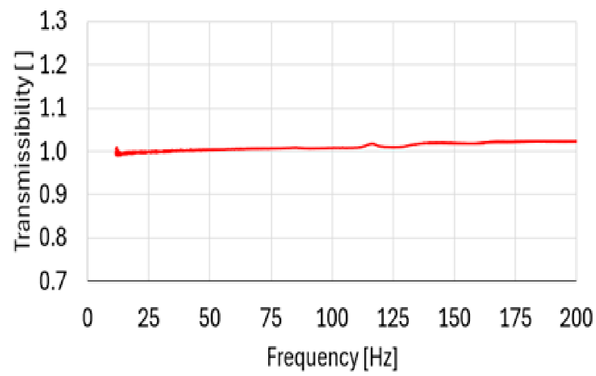

Fig. 10. Transmissibility Graph Occurs Using Bolt Fastening at Acceleration 8G

The resonance identified at a frequency of 28 Hz was further investigated and confirmed through additional graphical analyses. The author illustrated the relationship between frequency, acceleration, and displacement in Fig. 11.

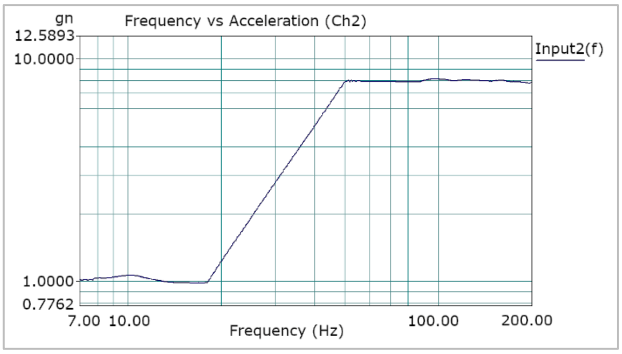

(a)

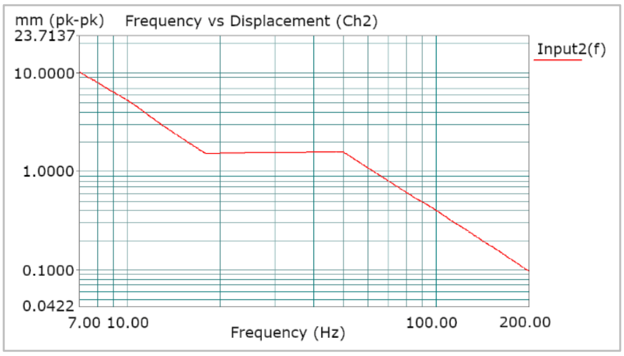

(b)

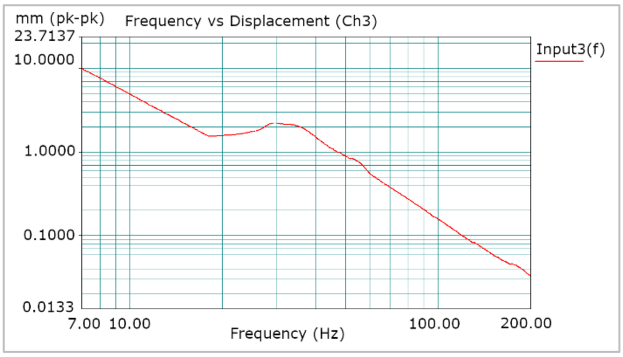

(c)

Fig. 11. (a) Plot Frequency vs Acceleration Graph of the second test
(b) Frequency vs Displacement Transducer Graph Plot 2 of the second test
(c) Frequency vs Displacement Transducer Graph Plot 3 of the second test

Figures 11 (b) and (c) indicate that the displacement should remain constant within a frequency range of 18 Hz to 50 Hz, specifically at a value of 1.5 mm. However, transducer 3 registered an increase at a frequency of 28 Hz, reaching approximately 2.2 mm. It creates a 2.2 – 15 mm gap, equivalent to 0.7 mm, denoted as the most critical value in Li-ion battery testing.

The global stiffness value of the battery spring structure can be predicted from these data. The stiffness value is obtained by dividing the sprung mass by the deflection that occurs.

$$k = \frac{F}{x}$$

$$k = \frac{sprung\ mass\ x\ acceleration}{displacement}$$

$$k = \frac{6.61\ kg\ x\ 34.335\ m/s^{-2}}{0.0007\ m}$$

$$k = 324220\ N/m$$

With four elastic foundations installed in each corner, the stiffness value of each elastic foundation is 81055 N/m. From this experimental data, the authors compare the experimental result with the available literature[25]. Figure 12 depicts a graph of deflection vs load.

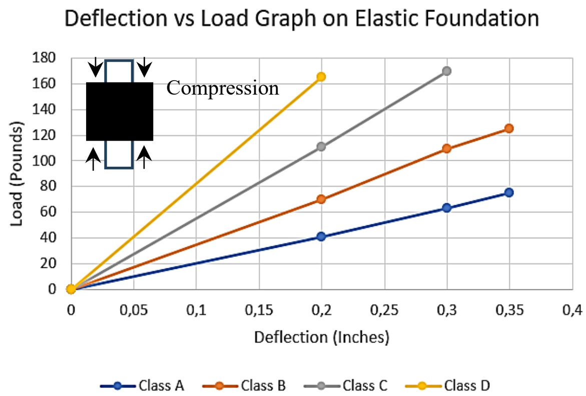

Fig. 12. Deflection vs Load graph on elastic foundation.

For a maximum load of 40 pounds (18.14 kg), the elastic foundation type with load range A is chosen, which can be interpreted as a load of around 6.61 kg (14.57 pounds). The elastic foundation load range Class A elastic foundation will deflect by 0.09 inches (0.002286 meters). Therefore, the stiffness value can be determined :

$$k = \frac{F}{x}$$

$$k = \frac{sprung\ mass\ x\ acceleration}{displacement}$$

$$k = \frac{6.61\ kg\ x\ 9.81\ m/s^{-2}}{0.002286\ m}$$

$$k = 28365\ N/m$$

These data show a gap in stiffness values between experimental results and literature studies. In further research, it is hoped that an in-depth analysis of why there is a difference in stiffness between the two data is carried out, where the literature stiffness value is 34% of the experimental stiffness value.

Natural frequency approach

Natural frequencies have the potential to amplify resonance. Resonance is not expected because it can disrupt the structural equilibrium system[32)33)34)]. The structure's natural frequency can be calculated with data availability: the spring's stiffness and the system's spring mass. By employing Equation 2, the natural frequency can be obtained as follows.

$$Wn = 0.5\,\pi^{-1}\left[\frac{k}{m}\right]^{0.5}$$

$$Wn = 0.5\,\pi^{-1}\left[\frac{28365\ N/m}{6.61\ kg}\right]^{0.5}$$

$$Wn = 10.42\ Hz \ \ \text{(literature value)}$$

The Wn value experimentally was found to be 28 Hz or when resonance occurs, while the Wn literature value was found to be 10.42 Hz or around 37.2% of the experimental Wn value, namely 28 Hz. As before, in further research, it is hoped that we can analyze in depth how to determine the Wn value of a battery structure that has a sprung mass configuration like the battery used in this research.[35)]

Furthermore, a sprung-mass structure is expected to protect the lithium-ion battery itself[36)]. The occurrence of resonance at the 28 Hz frequency proves that there is an imperfect gap in the battery protection. In battery vibration testing, the structure should be able to reduce all disturbances caused by the table shaker in all conditions ranging from frequencies of 7 - 200 Hz and accelerations of 1 - 8 G. With indications that no resonance occurs in all conditions. If the transmissibility graph plot is stated, the gn/gn value on transducer three should ideally be a maximum of 1, or the same as the input transducer, as is the case with transducer four, where the graph plot value is close to 1.

Physical Findings

Severe damage was reported due to seven vibration testing cycles, consisting of one swept test cycle and six original cycles. The findings of quite severe damage can be seen in the Fig.13. In Figure 13, referring to Fig. 1.b as mechanical arrangement, the elastic foundation breaks down the depressed leg BMS Holder. In terms of hardness value, the hardest component is the upper case, then continued with the BMS Holder leg, and the frailest is the elastic foundation. So, the elastic foundation is damaged the worst.

A study reported no mechanical damage observed when investigating the influence of vibration exposure on Li-Ion battery cell 18650[37)]. Compared with recent work, no contradictions were observed. In this study, we also found no damage to the battery cells. Please note that this study examines the direct impact of vibration on cells. A jig fixture was created to connect the cells directly, resulting in stronger vibrations compared to current methods. The current research methods are expected to cause less damage to battery cells.

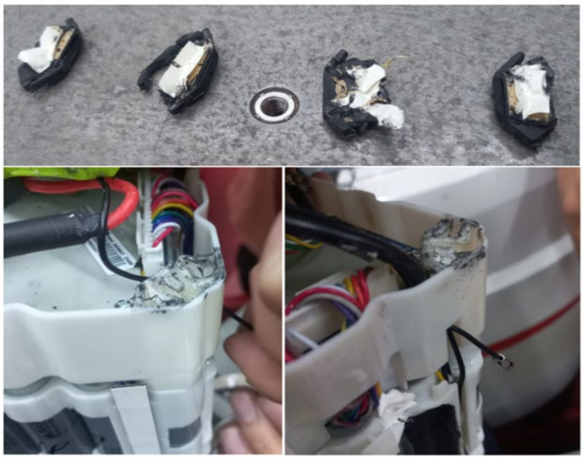

Fig. 13. Severe Damage to 4 Elastic Foundations and Damage to the BMS Holder

From Figure 13, it can be concluded that one swept test cycle with a frequency of 200 Hz and an acceleration of 1 G and six cycles of the UN ECE R136 vibration test with a frequency of 200 Hz and an acceleration of 8 G or half the total cycle is enough to destroy the elastic foundation which acts as a buffer to protect against vibrations experienced by the battery. More severe damage will certainly occur when the test is carried out for a total of 12 cycles. According to previous research, resonance frequencies can be eliminated by structural modification against vibration tests, modifications proposed by the thickness and length of material to avoid resonance frequencies[38)]. In a study mentioned that the installation of a rigid rubber bolt, 150 Ns / m produces a smaller displacement value, of 15 mm, compared to the installation of a rubber bolt that is medium 125 Ns / m with a displacement of 20 mm or soft 103 Ns / m with a displacement of 28 mm. This shows that more rigidity, a damping will result in a small displacement value[39)]. It is suggested that future research should include 12 testing cycles, as required by UN ECE R136. Additionally, there should be an emphasis on optimizing the design, particularly modifying the elastic foundation as a spring mechanism. The goal is to eliminate resonance frequencies during battery vibration testing.

4. Acknowledgement

MAF would like to thank the Head of the Research Center for Testing Technology and Standard BRIN for providing invaluable technical support during testing and data collection through the Research Student Internship Program 2023-2024.

5. Conclusion

Vibration testing on batteries has been demonstrated to induce structural damage, as extensively outlined in various previous studies. This research obtained a resonance frequency of 28 Hz on the battery pack, determined through direct experimental methods for battery testing according to UN ECE R136. Although the experimental value is slightly higher than the calculated value of 10.42 Hz, it remains significantly distant from the fixture's resonance frequency of 158 Hz. At the battery pack's resonance frequency, a disturbance force of 226.95 N is applied to the structure, smaller than the force experienced at peak frequency and peak acceleration, which is 171.18 N. Recognizing the potential for resonance to amplify disturbances, future efforts should concentrate on optimizing the structure to withstand resonance phenomena throughout the entire test series, spanning frequencies from 7 to 200 Hz and accelerations from 1 to 8 G. This optimization is crucial for minimizing interference with the battery cells.

Contributions

MAF prepared the test specimens and designed the fixture. MAF and HF constructed test set up and conducted the measurement. MAF analyzed the data and wrote the manuscript with support from NR and HF. NR and HF supervised the research program. All the authors discussed the results.

References

1) Indonesia Ministry of Finance, "Indonesia commitment in order net zero emission target," *Www.Kemenkeu.Go.Id*, 12–15 (2023). https://www.kemenkeu.go.id/informasi-publik/publikasi/berita-utama/Ini-Komitmen-Indonesia-Mencapai-Net-Zero-Emission (accessed November 1, 2023).
2) S. Permana, N. Trianti, and A. Rahmansyah, "Nuclear energy contribution for net zero emission and national energy mix 2060 in indonesia," *J. Phys. Conf. Ser.*, **2243** (*1*) (2022). doi:10.1088/1742-6596/2243/1/012066.
3) H. Andriansyah, and P. Ekadewi, "Indonesia Post-Pandemic Outlook : Strategy towards Net-Zero Emissions by 2060 from the Renewables and Carbon-Neutral Energy Perspectives," BRIN Publishing, Jakarta, 2022.
4) J. Santosa, A.H. Kuncoro, A. Dwijatmiko, N.W. Hesty, and A. Darmawan, "The role of nuclear power plants in indonesia towards net zero emissions (nze) in 2060 with a multi regions approach," *Evergreen*, **10** (*3*) 1660–1673 (2023). doi:10.5109/7151715.
5) A.S.S. Qalbie, and R. Rahmaniah, "The opportunity to achieve net zero emissions in indonesia through the implementation of a green economy to address climate change," *Glob. South Rev.*, **5** (*1*) 80 (2023). doi:10.22146/globalsouth.86381.
6) Nurdin P., "Penjualan mobil listrik naik 1.000 persen, terlaris hyundai ioniq 5," (2023). https://otomotif.kompas.com/read/2023/03/01/081200915/penjualan-mobil-listrik-januari-2023-ioniq-5-terlaris-geser-air-ev (accessed October 1, 2023).
7) C.S. Candra, "Evaluation of barriers to electric vehicle adoption in indonesia through grey ordinal priority approach," *Int. J. Grey Syst.*, **2** (*1*) 38–56 (2022). doi:10.52812/ijgs.46.
8) I. Veza, M.A. Abas, D.W. Djamari, N. Tamaldin, F. Endrasari, B.A. Budiman, M. Idris, A.C. Opia, F.B. Juangsa, and M. Aziz, "Electric vehicles in malaysia and indonesia: opportunities and challenges," *Energies*, **15** (*7*) (2022). doi:10.3390/en15072564.
9) D. Novizayanti, E.A. Prasetio, M. Siallagan, and S.P. Santosa, "Agent-based modeling framework for electric vehicle adoption transition in indonesia," *World Electr. Veh. J.*, **12** (*2*) (2021). doi:10.3390/wevj12020073.
10) N.M.A. Wijaya, I.N.S. Kumara, and Y. Divayana, "PERKEMBANGAN baterai dan charger untuk mendukung pemasyarakatan sepeda listrik di indonesia," *J. SPEKTRUM*, **8** (*1*) 15 (2021). doi:10.24843/spektrum.2021.v08.i01.p3.
11) ASEAN, "ASEAN Mutual Recognition Arrangement on Type Approval for Automotive Products," 2021.
12) United Nations, "Uniform provisions concerning the approval of vehicles of category l with regard to specific requirements for the electric power train," *Unece.Org*, 87 (2016).
13) M. Nizam, M.R.A. Putra, and Inayati, "Heat management on lifepo4 battery pack for eddy current brake energy storage on rapid braking processes," *Evergreen*, **9** (*2*) 451–456 (2022). doi:10.5109/4794171.
14) J.M. Hooper, D. Williams, K. Roberts-Bee, A. McGordon, P. Whiffin, and J. Marco, "Defining a vibration test profile for assessing the durability of electric motorcycle battery assemblies," *J. Power Sources*, **557** (2023). doi:10.1016/j.jpowsour.2022.232541.
15) P. Múčka, "Simulated road profiles according to iso 8608 in vibration analysis," *J. Test. Eval.*, **46** (*1*) 405–418 (2018). doi:10.1520/JTE20160265.
16) M. Agostinacchio, D. Ciampa, and S. Olita, "The vibrations induced by surface irregularities in road pavements - a matlab® approach," *Eur. Transp. Res. Rev.*, **6** (*3*) 267–275 (2014). doi:10.1007/s12544-013-0127-8.
17) International Standar Organitation, "Mechanical vibration — Road surface profiles — Reporting of measured data," 2016.
18) L. Zhang, Z. Ning, H. Peng, Z. Mu, and C. Sun, "Effects of vibration on the electrical performance of lithium-ion cells based on mathematical statistics," *Appl. Sci.*, **7** (*8*) (2017). doi:10.3390/app7080802.
19) J.M. Hooper, J. Marco, G.H. Chouchelamane, J.S. Chevalier, and D. Williams, "Multi-axis vibration durability testing of lithium ion 18650 nca cylindrical cells," *J. Energy Storage*, **15** 103–123 (2018). doi:10.1016/j.est.2017.11.006.

20) X. Hua, and A. Thomas, "Effect of dynamic loads and vibrations on lithium-ion batteries," *J. Low Freq. Noise Vib. Act. Control*, **40** (*4*) 1927–1934 (2021). doi:10.1177/14613484211008112.
21) P. Berg, M. Spielbauer, M. Tillinger, M. Merkel, M. Schoenfuss, O. Bohlen, and A. Jossen, "Durability of lithium-ion 18650 cells under random vibration load with respect to the inner cell design," *J. Energy Storage*, **31** (2020). doi:10.1016/j.est.2020.101499.
22) C. Mikolajczak, P. Michael Kahn, K. White, and R. Thomas Long, "Lithium-Ion Batteries Hazard and Use Assessment Final Report," Springer US, Boston, MA, 2011. doi:10.1007/978-1-4614-3486-3.
23) V. Trivedi, A. Saxena, M. Javed, P. Kumar, and V. Singh, "Design of six seater electrical vehicle (golf cart)," *Evergreen*, **10** (*2*) 953–961 (2023). doi:10.5109/6792890.
24) X. Li, Z. Huang, W. Hua, L. Rao, Y. Tian, and J. Tian, "Mechanical vibration modeling and characterization of a plastic-cased lithium-ion battery," *Green Energy Intell. Transp.*, **1** (*2*) (2022). doi:10.1016/j.geits.2022.100006.
25) M. Hussey, and H. Saunders, "Fundamentals of mechanical vibration," *J. Vib. Acoust.*, **108** (*4*) 482–483 (1986). doi:10.1115/1.3269379.
26) K. Ikeda, J. Kuroda, D. Uchino, K. Ogawa, A. Endo, T. Kato, H. Kato, and T. Narita, "Vibration characteristics control of resonance point in vehicle: fundamental considerations of control system without displacement and velocity information," *Vibration*, **6** (*1*) 1–10 (2023). doi:10.3390/vibration6010001.
27) D.J. Ewins, "Control of vibration and resonance in aero engines and rotating machinery - an overview," *Int. J. Press. Vessel. Pip.*, **87** (*9*) 504–510 (2010). doi:10.1016/j.ijpvp.2010.07.001.
28) H. Ding, E.H. Dowell, and L.Q. Chen, "Transmissibility of bending vibration of an elastic beam," *J. Vib. Acoust.*, **140** (*3*) (2018). doi:10.1115/1.4038733.
29) R. Deboli, A. Calvo, and C. Preti, "Whole-body vibration: measurement of horizontal and vertical transmissibility of an agricultural tractor seat," *Int. J. Ind. Ergon.*, **58** 69–78 (2017). doi:10.1016/j.ergon.2017.02.002.
30) M. Wnuk, and A. Iluk, "Estimation of resonance frequency for systems with contact using linear dynamics methods," *Appl. Sci.*, **12** (*18*) (2022). doi:10.3390/app12189344.
31) G. Ślaski, M. Spadło, J. Marcinkiewicz, and W. Konieczny, "Analysis and experimental tests of potential new mounting techniques for use in vibration testing of electric vehicle battery packs on electromagnetic exciters: advantages and disadvantages," *Appl. Sci.*, **14** (*7*) 2920 (2024). doi:10.3390/app14072920.
32) Hugh Young, and Roger Freedman, "University physics," *Phys. Today*, **3** (*1*) 5–39 (1950). doi:10.1063/1.3066770.
33) S.H. Ju, and H.T. Lin, "Resonance characteristics of high-speed trains passing simply supported bridges," *J. Sound Vib.*, **267** (*5*) 1127–1141 (2003). doi:10.1016/S0022-460X(02)01463-3.
34) A. Dijckmans, P. Coulier, J. Jiang, M.G.R. Toward, D.J. Thompson, G. Degrande, and G. Lombaert, "Mitigation of railway induced ground vibration by heavy masses next to the track," *Soil Dyn. Earthq. Eng.*, **75** 158–170 (2015). doi:10.1016/j.soildyn.2015.04.003.
35) A.K. Verma, and P.K. Saini, "Vibration model to detect local defect characteristics of deep groove ball bearing," *Evergreen*, **9** (*4*) 1056–1066 (2022). doi:10.5109/6625791.
36) G. Burshukova, A. Kanazhanov, R. Abuova, and A. Joldassov, "Analysis of using damping alloys to improve vibration and strength characteristics in the automotive industry," *Evergreen*, **10** (*2*) 742–751 (2023). doi:10.5109/6792824.
37) J.M. Hooper, J. Marco, G.H. Chouchelamane, and C. Lyness, "Vibration durability testing of nickel manganese cobalt oxide (nmc) lithium-ion 18,650 battery cells," *Energies*, **9** (*1*) 1–27 (2016). doi:10.3390/en9010052.
38) W.B. Jeong, W.S. Yoo, and J.Y. Kim, "Sensitivity analysis of anti-resonance frequency for vibration test control of a fixture," *KSME Int. J.*, **17** (*11*) 1732–1738 (2003). doi:10.1007/BF02983603.
39) M.F. Abdillah, B.A. Budiman, I.P. Prasetio, and P.L. Sambegoro, "Minimizing dynamic loading resonance of battery pack subjected to road profile loads," *IOP Conf. Ser. Mater. Sci. Eng.*, **1109** (*1*) 012012 (2021). doi:10.1088/1757-899x/1109/1/012012.